中國機械工程學刊第三十九卷第一期第 65~73 頁(民國一百零七年)
Journal of the Chinese Society of Mechanical Engineers, Vol.39, No.1, pp 65~73 (2018)

# Performance and Wear Characteristics of Cutting Tool in Laser Ultrasonically Assisted Cutting of Cemented Carbides

Chang-Juan Zhang*, Feng Jiao** and Ying Niu***

Keywords : cemented carbide, laser ultrasonically assisted cutting, ultrasonically elliptical vibration cutting, laser assisted cutting, tool wear.

## ABSTRACT

Laser ultrasonically assisted cutting (LUAC) for processing difficult-to-machine materials was proposed based on ultrasonically elliptical vibration cutting (UEVC) and laser assisted cutting (LAC), and experimentally compared with conventional cutting (CC), UEVC and LAC. The cutting performance of cemented carbides with different hardness using polycrystalline cubic boron nitride (PCBN) cutting tools was analyzed and wear mechanisms of the cutting tools was discussed by detecting tool wear conditions, cutting forces and surface morphology of workpiece and analyzing the energy spectrum of worn areas by scanning electron microscopy (SEM). The results showed that compared to CC, UEVC and LAC, LUAC showed significantly decreased cutting force, reduced tool wear, obviously prolonged tool life, and smoother surface quality of workpiece, especially for the cemented carbide with more cobalt elements. In addition, LUAC of cemented carbide was characterized by smooth and uniform crater on the rake face of the cemented carbide and narrow triangular wear land and shallow pits and scratches at the flank face of the cemented carbide. The failure mechanisms of PCBN cutting tool were the synergistic interaction among diffusive wear, adhesive wear, oxidation wear and abrasive wear.

*Paper Received May, 2016. Revised December, 2016. Accepted January, 2017. Author for Correspondence: Chang-Juan Zhang.*

* *Associate Professor, School of Mechanical and Power Engineering, Henan Polytechnic University, Jiaozuo, Henan, China*

** *Professor, School of Mechanical and Power Engineering, Henan Polytechnic University, Jiaozuo, Henan, China*

*** *Ph.D student, School of Mechanical and Power Engineering, Henan Polytechnic University, Jiaozuo, Henan, China*

## INTRODUCTION

Cemented carbide is an important tool and structural material. Because of its excellent properties such as high hardness and toughness, it has been widely used in metallurgy, machinery, petroleum and mine industries. Its relatively high wear resistance and chemical stability also set it apart from other counterpart materials (Konyashin, 2015; Amartya, 2011). However, cemented carbide is hard to machine owing to its high brittleness and low facture toughness that would lead to severe cutting tool wear and high processing cost. As a result, using traditional processing methods is difficult to meet the requirements of precision and ultra-precision machining of cemented carbide. In addition, although powder preparation of cemented carbide and performance of cemented carbide cutting tools have been previously studied (Stanciu, 2016; Tsai, 2016; Katiyar, 2016), very few investigations have focused on the precision and ultra-precision machining of cemented carbide.

Ultrasonically assisted machining is a non-conventional machining technique that employs superposition of high frequency and low amplitude vibrio-impacts on the cutting tools. In recent years, a significant amount of work on ultrasonically elliptical assisted machining has been carried out to investigate its machining mechanism and cutting system. Previous reports (Patil, 2014; Cong, 2014; Zhang, 2014; Yu, 2016) have shown that ultrasonic vibration cutting could significantly reduce the cutting force and temperature in machining of difficult-to-machine materials, extend the lifespan of cutting tool and improve surface quality of the workpiece.

Over the last few decades, researchers have successfully demonstrated the advantages of hot machining where the workpiece material was pre-heated to improve its machinability. The principle of this technique is based on the temperature-dependence of shear strength of high strength materials. Because heating could soften the workpiece material, the material removal is improved and the cutting tool wear is reduced. Previous studies (Lajis, 2009; Amin, 2008; Germain, 2011) have utilized various types of localized and bulk heating sources for thermal softening of the workiece materials in hot machining. Thereinto, laser assisted machining is successfully applied to precision machining of difficult-to-machine materials owning to its superior performances, such as flexible control, and the ability to emit and adjust laser spot with accurate size and shape. Wang et al (2003) , have used the physical model in laser assisted cutting of $Al_2O_3$ particle reinforced Al-matrix composite materials to reduce cutting force and tool wear and to improve cutting surface mechanics performance. WU et al (2010) explored the effect of machining parameters on cutting forces and specific cutting energy, and analyzed the forms and causes of tool wear in laser assisted machining of silicon nitride ceramics. Bejjania et al (2011) studied the tool wear characteristics in laser assisted turning of titanium metal matrix composite materials and found that laser assisted machining could increase tool life by up to 180%. Anderson et al (2006) evaluated the machinability of Inconel 718 with carbide and ceramic inserts using conventional and laser assisted machining methods and showed that compared with conventional machining, laser assisted machining could improve surface roughness by 2-3 fold and ceramic tool life by 200-300%.

However, the heat stress produced in the process of hot machining of difficult-to-machine materials could generate microcracks on the surface of workpiece, thereby reducing the surface quality and increasing the processing cost. Therefore, hot machining technique was often utilized in combination with ultrasonic vibration machining to form a new hybrid machining process called hot ultrasonically assisted machining. Although the technique has been applied in high efficient and precise machining of difficult-to-machine materials, very few results have been reported. Hsu et al(2008) investigated the machining characteristics of Inconel 718 using ultrasonic and high temperature-aided cutting and found that application of ultrasonic vibration cutting in the tangential direction could reduce surface roughness of workpiece and cutting force and prolong service life of the cutter. Muhammad et al (2012; 2013; 2014) experimentally and numerically studied the hot ultrasonically assisted turning of Ti alloy and demonstrated reduction in the cutting forces and improvement in surface roughness. Overall, most studies are mainly focused on the cutting force and surface quality in hot ultrasonically assisted machining of difficult-to-machine materials. But the tool wear mechanism has not been comprehensively investigated. Moreover, the heat sources in hot ultrasonically assisted machining were gas torch, heater, etc, and researches on laser ultrasonically assisted machining are very scarce. In addition, the tool wear is very severe and complex in laser ultrasonically assisted machining of cemented carbide, which would cause greater machining errors of workpiece and greatly affect the processing efficiency and machining cost. Therefore, researches on tool wear characteristics in laser ultrasonically assisted machining of cemented carbide are of significance and necessity.

In this work, laser ultrasonically assisted cutting (LUAC) was proposed by combining ultrasonically elliptical vibration cutting (UEVC) and laser assisted cutting (LAC), and compared with conventional cutting (CC), UEVC and LAC by examining their tool wear in producing different cemented carbides using polycrystalline cubic boron nitride (PCBN) tools on an ultra-precision lathe. In addition, the cutting performance and wear mechanism of PCBN cutting tools were also investigated.

## PRINCIPLE OF LUAC

As shown in Fig 1, the workpiece was subjected to rotary movement with speed of $n$ and the cutting tool was subjected to feeding movement along the radial direction with speed of $v_f$ . The high power laser beam was focused on the workpiece surface in front of the tool edge, and the local surface was heated to very high temperature in a short period of time to change the material machinability and soften the workpiece. Meanwhile the cutting tool was exerted to ultrasonic vibration with the same frequency at both tangential and radial directions to realize the ultrasonically elliptical vibration cutting of the softened workpiece, avoid the longtime friction between the tool flank face and the machined workpiece surface, and reduce the cutting tool's edge breakage and its negative impact on the workpiece surface quality. Therefore, the tool wear would be reduced and the surface quality of workpiece would be improved by making the most of the advantages of laser assisted cutting and ultrasonically elliptical vibration cutting techniques when they are used in combination with each other.

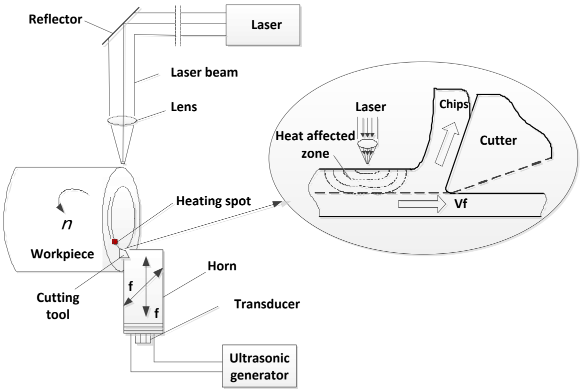


Fig. 1 Schematic diagram of LUAC.

## EXPERIMENTAL WORK

### Experimental Setup

The LUAC experimental setup consisted of an ultra-precision cutting system (ultra-precision CNC lathe), an acoustic vibration device and a laser heating device, as shown in Fig 2.

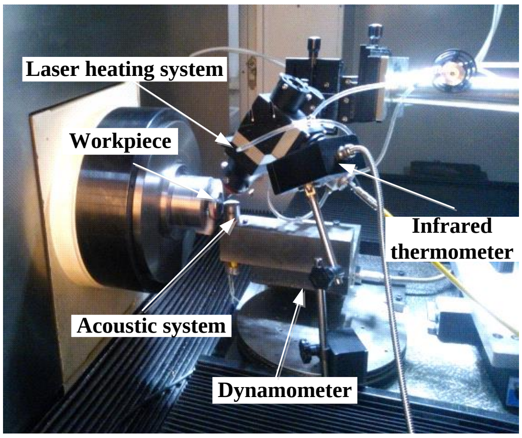


Fig. 2 Experimental setup.

The acoustic vibration device was composed of ultrasonic generator, transducer, horn and cutting tool. The laser heating device included a laser host, a laser power supply, a cooling system, a laser positioning system, an optical fiber transmission system and a laser focus device. The laser focus device connected to laser host through optical fibers was fixed on the machine table using the brackets. The laser spot and tool nose were kept with some distance through adjusting laser position and angle. Figure 3 shows that the two-dimensional longitudinal and flexural composite elliptical vibration of the cutting tool could be realized through the ultrasonic vibration system. According to the size of the cutting tool, a corresponding groove was processed at the top of the horn through the machining center, and the cutting tool was fixed on the horn with the screws. During the experiment, the ultrasonic device and the dynamometer used to record cutting forces in real time were bolted together on the machine table to synchronize the ultrasonic vibration device and the laser heating device. The experimental parameters are summarized in Table 1.

### Workpiece Materials and Cutting Tools

Cylindrical bars of YG10, YG15, YG20 and YG30 cemented carbides with initial diameter of 49mm and cobalt content of 10%, 15%, 20% and 30%, respectively, were used in the experiments. For all experiments, the diamond-shaped PCBN cutting blades with side length of 7mm were employed. Table 2 shows its geometry parameters.

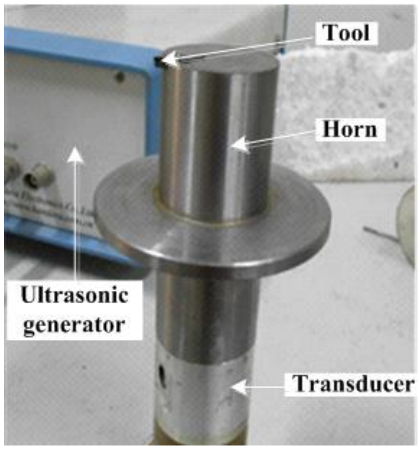


Fig. 3 Ultrasonic vibration system.

Table 1. Cutting parameters used in experiments.

| | |
|---|---|
| Cutting speed | 15m/min |
| Depth of cut | 10μm |
| Feed rate | 0.01mm/r |
| Laser wavelength | 1.06μm |
| Laser spot diameter | 0.8 mm |
| Laser incident angle | 60° |
| Laser power | 350 W |
| Distance between laser spot and tool nose | 2.5 mm |
| Ultrasonic vibration frequency | 35 kHz |
| Ultrasonic tangential amplitude | 1.4μm |
| Ultrasonic axial amplitude | 2.1μm |

Table 2. Cutting tool geometry.

| | |
|---|---|
| Rake angle | 0° |
| Clearance angle | 7° |
| Inclination angle | 0° |
| Edge angle | 62.5° |
| Nose radius | 0.8 mm |
| Nose angle | 55° |
| Negative land angle | 20° |
| Negative land width | 0.15 mm |

### Experimental Methods

Some studies have shown that the hardness of cemented carbide would be reduced drastically and the workpiece material would be softened when the cutting temperature is higher than 400ºC (Milman, 2002; Buss, 2004). Figure 4 shows the temperature field distributions of workpiece heating area with the turning conditions listed in Table 1. Meanwhile, the average temperature of the laser spot center on the workpiece surface and the tool nose measured using an infrared thermometer was about 665ºC and 410ºC, respectively. With thus temperature, the cutting performances of cemented carbide were improved without affecting the tool life. Therefore, the CC and UEVC experiments were carried out at room temperature, while the LAC and LUAC experiments were carried out at cutting zone temperature of about 410℃. In order to reduce the influence of tool setting errors on the subsequent tool wear, a tool auto-checking instrument was used in the experiments. In addition, three cutting tools with the same geometric parameters were used in each of CC, UEVC, LAC and LUAC experiment and the tools were retracted when the workpiece diameter shortened to 37 mm. The tool flank wear was measured by using three-dimensional digital microscope with KEYENC VHX-2000C and SEM. The average tool wear of the three cutting tools in CC, UEVC, LAC and LUAC was obtained and the energy spectrum of worn areas was analyzed. In addition, the surface morphology was detected using white light interferometer.

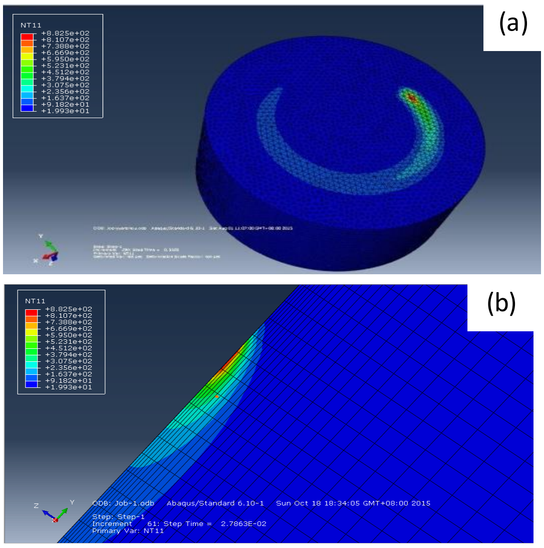


Fig.4 Temperature distribution (a) on surface of the workpiece and (b) in vertical section of the workpiece.

## EXPERIMENTAL RESULTS AND DISCUSSION

### Tool Wear Characteristics

The flank wear curves of YG20 cemented carbide in CC, UEVC, LAC and LUAC are shown in Fig 5. It is clear that all wear curves can be divided into initial, normal and acute worn stages but different nodes. The nodes of the initial, normal and acute worn stages were the cutting distances of 0-150 m, 150-450 mm and beyond 450 mm, respectively, in CC; 0-180 m, 180-600 mm and beyond 600 mm, respectively, in UEVC; 0-200 m, 200-650 mm and beyond 650 mm, respectively, in LAC; and 0-200 m, 200-975 mm and beyond 975 mm, respectively, in LUAC. In addition, a substantial decrease of the flank wear of LUAC compared with CC, UEVC and LAC was observed with the cutting distance increasing. Compared to CC, the smaller tool flank wear was also obtained in other three cutting conditions, showing minimum in LUAC. Meanwhile, as the cutting distance increases, the tool flank wear in CC, UEVC, LAC and LUAC also increases but at different wear rate at each worn stage. At the initial worn stage, the wear rates were different among CC, UEVC, LAC and LUAC, at the normal worn stage, the wear rates in UEVC and LAC were basically the same, and at the acute worn stage, the wear rates increased rapidly in CC, UEVC and LAC, but steadily in LUAC.

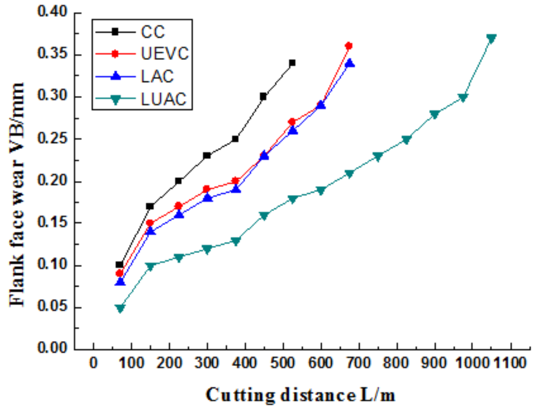


Fig. 5 Relationship between tool flank wear and cutting distance.

Figure 6 indicates the tool flank wear of different cemented carbides in LUAC. When the workpiece materials were YG10, YG15, YG20 and YG30 cemented carbides, the content of cobalt increased gradually, resulting in the decrease of workpiece hardness and the tool wear.

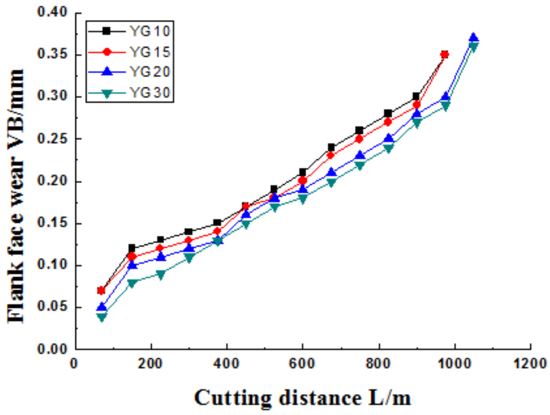


Fig. 6 Tool wear characteristics in LUAC of different cemented carbides.

### Tool Wear Patterns

The digital microscope photographs of the flank wear of YG20 cemented carbides in CC, UEVC, LAC and LUAC with the cutting distance gradually increasing are shown in Fig 7. It can be found that the triangular wear land was formed on the flank face. At cutting distance of 283.4m, the flank wear lands in CC and LAC were covered with obvious micro-grooves oriented along the cutting direction, making the tool wear more serious. However, the tool wear was less and the flank wear lands were narrower and smoother in UEVC and LUAC. At this time the tool wear was at the initial worn stage.

When the cutting distance increased to 368.3m, the flank wear zone was smooth and uniform and the width of the wear land increased. In CC, the length and width of the wear zone increased significantly. In UEVC, the crater wear near the tool edge was formed on the rake face. In LAC, the depth of the micro-groove near tool edge increased. And in LUAC, the quality of the flank face was still fine. At this time, the tool wear was at the normal worn stage.

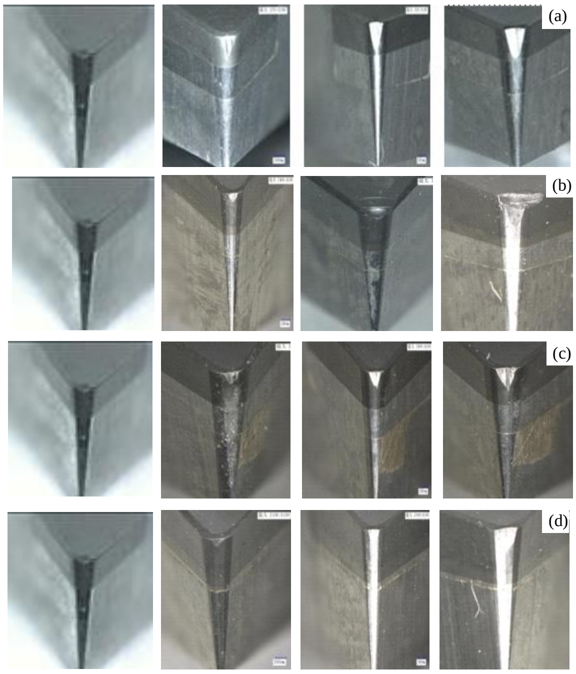


Fig. 7 Tool wear morphologies at different cutting distances of 0, 283.4, 368.3 and 584.4 m from left to right, respectively, in (a) CC, (b) UEVC, (c) LAC and d) LUAC

Figures 8 and 9 show the tool wear morphologies of flank face and rake face of YG20 cemented carbide at the cutting distance of 584.4 m. It can be seen that the width of the wear land in CC, UEVC, LAC and LUAC gradually decreased. Furthermore, the number and depth of micro-grooves on the wear land also decreased. In CC, obvious crater wear, brittle delamination near the tool edge on the rake face, and severe flank wear land were found, and the tool wear was the most serious. In UEVC, sheet delamination near the tool edge on the rake face was found due to the high frequency intermittent impact. In LAC, the tipping near the tool edge was found and the depth of the microgroove on the flank wear land increased. At this time, the tool wear was still at the normal worn stage in LUAC, but already at the acute worn stage in CC, UEVC and LAC.

Figures 10 and 11 compared the aggravation in tool crater wear and flank wear of YG10 and YG20 cemented carbides. The width and depth of the crater on rake face of YG10 cemented carbide were more serious and the number and depth of the grooves on flank face of YG10 cemented carbide also increased. Especially, the tool wear near the tool edge was the most serious.

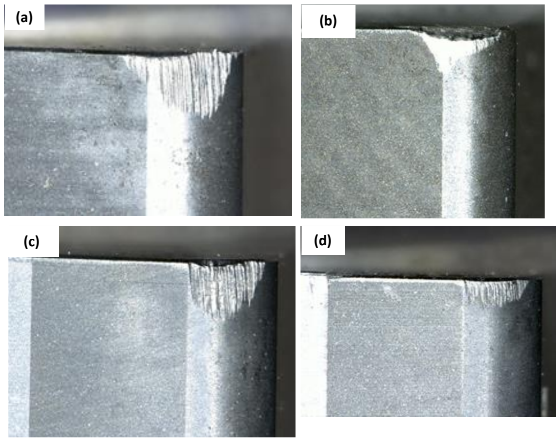


Fig. 8 Tool wear morphologies on flank face of YG20 cemented carbide at cutting distance of 584.4 m in (a) CC, (b) UEVC, (c) LAC and (d) LUAC.

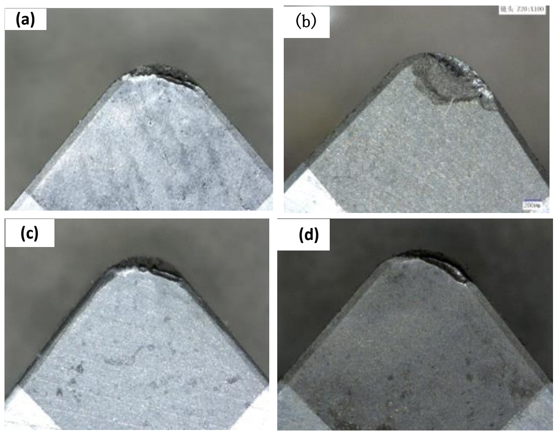


Fig. 9 Tool wear morphologies on rake face of YG20 cemented carbide at cutting distance of 584.4m in (a) CC, (b) UEVC,(c) LAC,(d) LUAC.

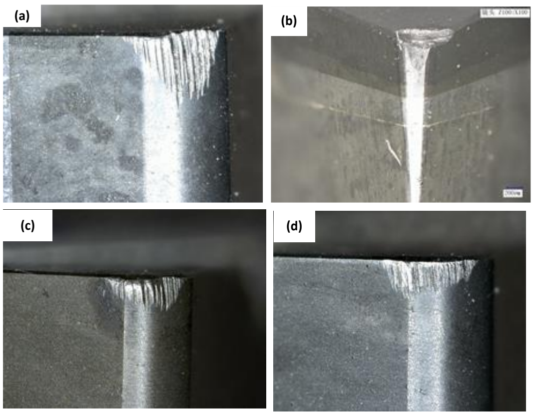


Fig. 10 Tool wear morphologies on flank face of YG10 cemented carbide at cutting distance of 584.4 m in (a) CC, (b) UEVC, (c) LAC and (d) LUAC.

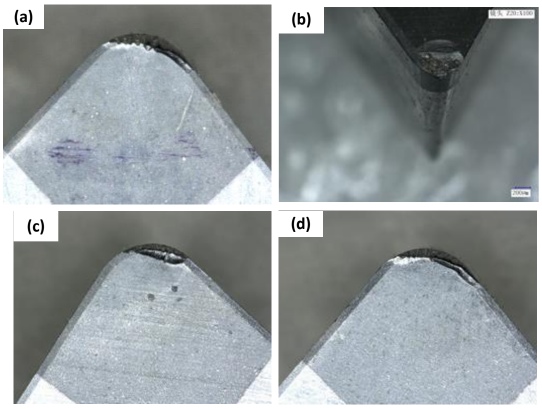


Fig. 11 Tool wear morphologies on rake face of YG10 cemented carbide at cutting distance of 584.4 m in (a) CC, (b) UEVC, (c) LAC and (d) LUAC.

Discussion

Figure 12 shows that the gradually increased cutting force of YG20 cemented carbide at different cutting distances in CC, UEVC, LAC and LUAC and Figure 13 shows the cutting force of different cemented carbides at different cutting distances in LUAC. Figure 14 shows the surface morphology of workpiece of YG20 cemented carbide at different cutting distances in CC, UEVC, LAC and LUAC, and Figure 15 shows the surface morphology of workpiece of different cemented carbides at different cutting distances in LUAC.

It can be found that in UEVC, the tool separated from the workpiece during the relaxation stage of each cycle of vibration, resulting in the reduction of cutting force and the improvement of surface quality of workpiece. In LAC, the cutting force was lower and the surface quality of workpiece was better owing to the thermal softening of the workpiece material. Therefore, in LUAC, the cutting force was the minimum and the surface quality of workpiece was the best because of the combined actions of ultrasonic intermittent contact and thermal softening. In Fig 13 and Fig 15, with the hardness of workpiece materials reducing from YG10, YG15, YG20 to YG30 cemented carbides, the shear stress during cutting also reduced, leading to the decrease of cutting force and tool wear and improvement of surface quality of workpiece.

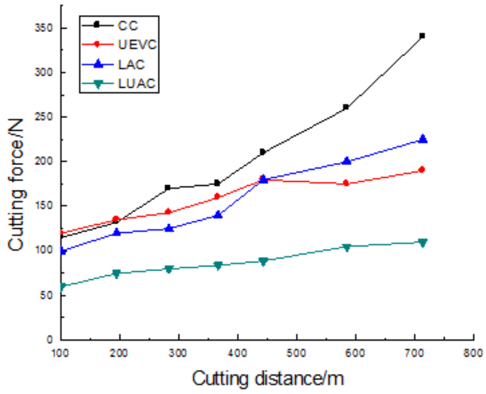


Fig. 12 Cutting forces of YG20 cemented carbide at different cutting distances.

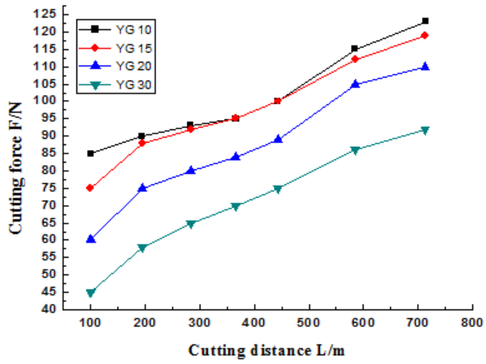


Fig. 13 Cutting forces of different cemented carbides at different cutting distances.

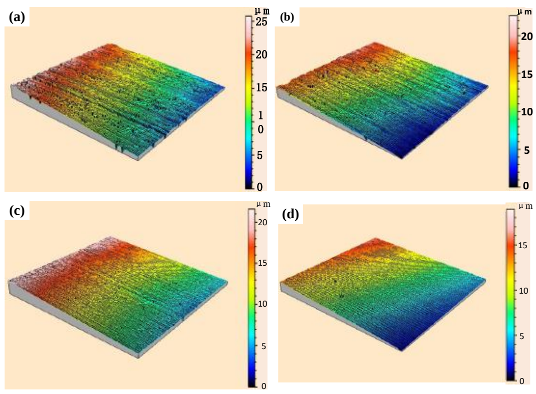


Fig.14 Surface morphology of YG20 cemented carbide in (a) CC, (b) UEVC,(c) LAC,(d) LUAC.

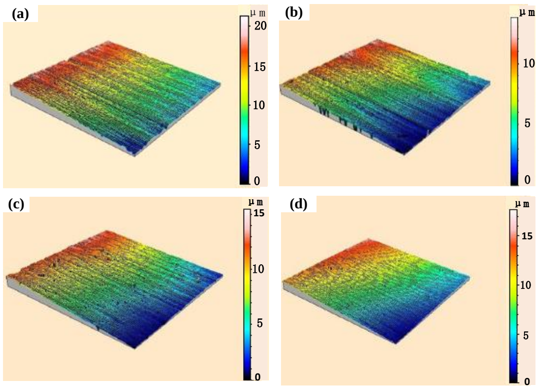


Fig.15 Surface morphology of different cemented carbides in LUAC in (a) YG10, (b) YG15,(c) YG20,(d) YG30.

At the initial and normal worn stages, tools were sharp and have good heat conductivity. Therefore, the increase of tool wear in CC, UEVC, LAC and LUAC was steady. In CC, the larger cutting force and heat loss due to continuous contact between tool and workpiece also led to severe tool wear. In UEVC and LAC, the smaller cutting forces led to reduction of tool wear. Therefore, with the advantages of ultrasonically vibration and laser heating, the tool wear was significantly reduced and the tool lifetime was prolonged.

At the acute worn stage, the sharpness of the tool was impaired and the contact area between workpiece and tool increased, leading to significant increase in the cutting force, temperature and tool wear. Compared with that in UEVC, the tool wear was more serious in LAC due to larger plastic deformation of workpiece. However, the tool wear in LUAC increased steadily because it was still at the normal worn stage.

At the beginning of the experiments, the stresses on the tool edge were very severe because the tool was new and sharp. Moreover, the negative rake angle (-20° in this paper) of the PCBN tools greatly increased the cutting force and temperature. Therefore, the rake face endured much higher pressure and temperature than the flank face, especially on the regions near the tool edge. Under such conditions, diffusive wear and oxidation wear would be the predominant wear patterns on the rake face. As the increase of the cutting distance, the tool wear increased gradually and the sharpness and the integrity of tool edge reduced, resulting in decreased stress concentration near the tool edge. In addition, small cutting parameters, high hardness and low plasticity of workpiece material made chips unable to exist on the rake face. Therefore, the effect of chip flow on the rake face was not obvious. However, the PCBN material is composed of many tiny and nondirectional CBN single crystals. Thus, their strength at the grain boundary was low and their actual strength was far below the theoretical strength. Thus, under the action of cutting force, tiny crystal particles near tool edge fell off, tool tipping formed, and a number of CBN grains spalled.

In the experiments, extrusion, friction, elastic recovery and relative motion between the machined surface of workpiece and the flank face of tool all led to the complicated interaction and higher cutting temperature. At the beginning of the experiment, because of the good sharpness of the cutting tool, the real contact area and the cutting force between the machined surface and the flank face were smaller. However, since the PCBN tool was made of CBN grains, which were sintered together with binding phase, the flank face of the tool was scratched and lapped by the hard particles in cemented carbide, resulting in the wear of the metal material cobalt as binding phase and the spall of the CBN grains. Therefore, the flank wear of the tool was formed due to abrasive wear, resulting in the wear land distributed with different degree of dents and grooves on the flank face. As cutting distance increases, the real contact region and the flank wear increase gradually that would reduce the actual relief angle. Furthermore, the chip flow was almost along and close to the flank face due to negative rake angle of the PCBN tools. Therefore, the cutting force acted to flank face of tool was significantly increased, the flank wear was aggravated, and the dents, grooves and spots on flank face were more severe.

Table 3 and Figure 16 show the chemical compositions of the tool flank worn zone in mass fraction using SEM when cutting YG20 cemented carbide. It can be seen that a large number of tungsten element was found in the tool flank race, especially in CC and LAC. In addition, the mass fraction of carbon and cobalt also changed, suggesting the presence of diffusive wear in CC, UEVC, LAC and LUAC of cemented carbide utilizing PCBN tools. Therefore, the inertia of CBN reduced and the affinity of CBN as the alloying elements increased. As the cutting force and temperature of cutting tool, chip and workpiece reached certain values, the adhesive wear of the cutting tool was formed, and the nickel elements of the cutting tool would further enhance the adhesive strength and aggravate the adhesive wear, leading to the tipping of the tool edge. Meanwhile, the increased content of oxygen element in LAC and LUAC also indicated that with temperature increasing, cobalt element would react chemically with oxygen element and nitrogen element would be replaced, resulting in continuous oxide film formation and polishing by the chill layer, hard points in workpiece surface, as well as oxidation wear of tools. In UEVC and LUAC, under high frequent and intermittent impact, the contents of titanium, and aluminum elements decreased significantly, leading to the occurrence of abrasive wear at different degree.

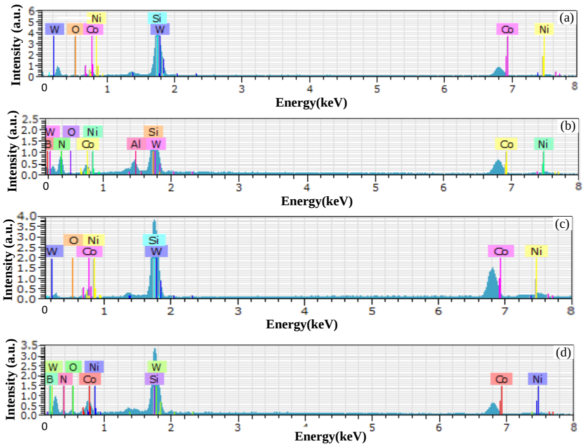

Fig.16 Chemical composition of flank worn zone in (a) CC, (b) UEVC,(c) LAC,(d) LUAC.

Table 3. Chemical composition of flank worn zone.

| | Elements content （%） | | | | | | |
|---|---|---|---|---|---|---|---|
| | W | N | Co | C | Ti | Al | O |
| CC | 43.61 | 20.49 | 13.61 | 8.33 | 5.27 | 3.62 | 3.11 |
| UEVC | 21.35 | 19.10 | 17.89 | 13.09 | 1.04 | 2.27 | 2.96 |
| LAC | 36.18 | 15.28 | 17.64 | 12.28 | 5.60 | 2.93 | 5.82 |
| LUAC | 27.26 | 22.48 | 24.13 | 10.80 | 1.24 | 2.82 | 6.28 |

Overall, PCBN tool wear during the cutting of cemented carbide is a result of combined mechanical and thermochemical effects. The tool wear is mainly caused by actions of abrasion, diffusion and adhesion in CC, actions of abrasion and diffusion in UEVC, and combined actions of diffusion, adhesion and oxidation in LAC. But in LUAC, tool wear is caused by the synergistic interactions of diffusion, adhesion, oxidation and abrasion.

## CONCLUSIONS

(1) The cutting force and the tool wear in laser ultrasonically assisted cutting (LUAC) were reduced significantly when compared to conventional cutting (CC), ultrasonically elliptical vibration cutting (UEVC) and laser assisted cutting (LAC), and a remarkable extension in lifetime of tool was observed in LUAC. Therefore, the surface quality of the machined workpiece was improved in LUAC.

(2) The cutting force and the tool wear of cemented carbides were decreased with its cobalt content increasing and the tipping of the tool edge and the tool breakage were less likely to happen in cemented carbides with its cobalt content increasing. Therefore, PCBN cutting tool was more suitable for cutting cemented carbide with higher cobalt content.

(3) The tool wear on rake face in CC and UEVC of cemented carbide was characterized by brittle spall and exfoliation, respectively. The tool tipping was found in LAC. Smooth and uniform crater could be seen on tool rake face in LUAC. In addition, although triangular wear land and pits and scratches on the flank face were seen in each cutting mode, the wear land was narrower and the scratches were shallower in LUAC.

(4) PCBN tool wear occurred in cutting of cemented carbides is chiefly attributed to comprehensive actions of mechanical friction and thermochemical reaction. In particular, the main mechanisms of inducing tool wear in LUAC of cemented carbide are diffusive wear, adhesive wear, oxidation wear and abrasive wear.

## ACKNOWLEDGMENT

This research is supported by National Natural Science Foundation of China (No. 51075127), Henan Research Program of Fundamental and Frontier Technology (No. 152300410102) and Henan Provincial Key Discipline.

## REFERENCES

Konyashin, I. and Klyachko L.I., “History of cemented carbides in the Soviet Union,” *International Journal of Refractory Metals and Hard Materials*, Vol.49, pp.9-26 (2015).

Amartya M. and Bikramjit B., “Recent developments on WC-based bulk composites,” *Journal of Materials Science*, Vol.46, No.3, pp.571-589 (2011).

Stanciu, V. I., Vitry, V. and Delaunois, F., “Tungsten carbide powder obtained by direct carburization of tungsten trioxide using mechanical alloying method,” *Journal of Alloys and Compounds*, Vol.659, pp. 302-308 (2016).

Tsai M.Y., Chang S.Y., Hung J.p. and Wang C.C., “Investigation of milling cutting forces and cutting coefficient for aluminum 6060-T6,” *Computers & Electrical Engineering*, Vol.51, pp.320-330 (2016).

Katiyar, P. K., Singh, P.K., Singh, R. and Kumar A. I., “Modes of failure of cemented tungsten carbide tool bits (WC/Co): A study of wear parts,” *International Journal of Refractory Metals and Hard Materials*, Vol.54, pp. 27-38 (2016).

Patil S., Joshi S., Tewari A. and Joshi S.S., “Modelling and simulation of effect of ultrasonic vibrations on machining of Ti6Al4V,” *Ultrasonics*, Vol.54, No.2, pp.694-705 (2014).

Cong W. L., Pei Z. J., Sun X. and Zhang C.L., “Rotary ultrasonic machining of CFRP: A mechanistic predictive model for cutting force,” *Ultrasonics*, Vol.54, No.2, pp. 663-675 (2014).

Zhang, J.G., Suzuki, N. and Wang, Y.L., "Fundamental investigation of ultra-precision ductile machining of tungsten carbide by applying elliptical vibration cutting with single crystal diamond," *Journal of Materials Processing Technology*, Vol.214, pp.2644-2659 (2014).

Yu K.N., Wang C.C., Yau H.T. and Chen J.L., "Numerical computation and nonlinear dynamic analysis of ultrasonic cutting system," *Computers & Electrical Engineering*, Vol.51,pp.270-283 (2016).

Lajis M.A., Amin A.K.M.N., Karim A.N.M., Radzi H.C.D.M. and Ginta T.L., "Hot machining of hardened steels with coated carbide inserts," *American Journal of Engineering and Applied Sciences*, Vol.2, No.2, pp.421-427 (2009).

Amin A.K.M. N., Dolah S. B., Mahmud M. B. and Lajis M.A., "Effects of workpiece preheating on surface roughness, chatter and tool performance during end milling of hardened steel D2," *Journal of Materials Processing Technology*, Vol.201, No.1-3, pp.466-470 (2008).

Germain G.., Santo P. D. and Lebrun J. L., "Comprehension of chip formation in laser assisted machining," *International Journal of Machine Tools and Manufacture*, Vol.51, No.3, pp. 230-238 (2011).

Wang Y., Yang L.J. and Qi L.T., "Laser-assisted hot cutting characteristics of A l2O3 particle reinforced A l-matrix composite," *China Mechanical Engineering*, Vol.14, No.4, pp.344-346 (2003).

Wu X.F., Wang Y. and Zhang H.Z., "Experimental research on laser assisted machining of silicon nitride ceramics," *Journal of Astronautics*, Vol.31,No.5,pp.1457-1462 (2010).

Bejjani R., Shi B., Attia H. and Balazinskia M., "Laser assisted turning of Titanium Metal Matrix Composite," *CIRP Annal-Manufacturing Technology*, Vol.60, No.1, pp.61-64 (2011).

Anderson M., Patwa R. and Yung C. S., "Laser-assisted machining of Inconel 718 with an economic analysis," *International Journal of Machine Tools and Manufacture*, Vol.46, No.14, pp.1879-1891 (2006).

Hsu C.Y., Lin Y.Y., Lee W.S. and Lo S.P., "Machining characteristics of Inconel 718 using ultrasonic and high temperature-aided cutting," *Journal of Materials Processing Technology*, Vol.198, No.1-3, pp.359-365 (2008).

Muhammad R., Roy A. and Silberschmidt V. V., "Finite Element Modelling of Conventional and Hybrid Oblique Cutting Processes of Titanium Alloy," *Procedia CIRP*, Vol.8, pp.510-515 (2013).

Muhammad R., Maurotto A., Roy A. and Silberschmidt V. V., "Hot ultrasonically assisted cutting of β-Tialloy," *Procedia CIRP*, Vol.1, pp.336-341 (2012).

Muhammad R., Maurotto A., Demiral M. and Roy A., "Thermally enhanced ultrasonically assisted cutting of Ti alloy," *CIRP Journal of Manufacturing Science and Technology*, Vol.7, No.2, pp. 336-341 (2014).

Milman Y.V., Luyckx S., Goncharuck V.A. and Northrop J.T., "Results from bending tests on submicron and micron WC-Co grades at elevated temperatures," *International Journal of Refractory Metals and Hard Materials*, Vol.20, No.1, pp.71-79 (2002).

Buss, K. and Mari, D., "High temperature deformation mechanisms in cemented carbides and cermets studied by mechanical spectroscopy," *Materials Science and Engineering A*, Vol.370, pp.163-168 (2004).

# 硬質合金鐳射超聲輔助切削刀具性能及磨損特性

張昌娟　焦 鋒　牛 贏
河南理工大學機械與動力工程學院

## 摘 要

本研究基於鐳射加熱輔助切削和超聲振動切削提出了鐳射超聲輔助切削加工工藝，採用 PCBN 刀具對不同的硬質合金材料進行了普通切削，超聲振動切削，鐳射加熱輔助切削和鐳射超聲輔助切削對比試驗，對刀具磨損、切削力，工件表面形貌及刀具磨損區域的能譜進行了分析，對鐳射超聲輔助切削不同硬質合金材料時 PCBN 刀具的性能及磨損機理進行了研究。結果表明與普通切削、超聲振動切削及鐳射加熱輔助切削相比，鐳射超聲輔助切削過程中切削力減小，刀具磨損程度降低，工件表面品質提高；特別是鐳射超聲輔助切削鈷含量較高的硬質合金材料時，工件表面更加平整光滑，刀具使用壽命顯著提高。此外，採用 PCBN 刀具鐳射超聲輔助切削硬質合金時，刀具前刀面磨損呈現平滑且均勻的月牙窪，後刀面磨損呈現較窄的三角形磨損帶和較淺的凹坑和劃痕，擴散磨損、粘接磨損、氧化磨損和磨粒磨損共同導致了PCBN 刀具的磨損。